

**Strong and radiative decays of heavy flavored baryons**M. A. Ivanov <sup>\*</sup>, J. G. Körner <sup>†</sup>, V. E. Lyubovitskij <sup>\*‡</sup> and A. G. Rusetsky <sup>\*§\*\*</sup><sup>\*</sup> *Bogoliubov Laboratory of Theoretical Physics,  
Joint Institute for Nuclear Research, 141980 Dubna, Russia*<sup>†</sup> *Johannes Gutenberg-Universität,  
Institut für Physik, D-55099 Mainz, Germany*<sup>‡</sup> *Department of Physics,  
Tomsk State University, 634050 Tomsk, Russia*<sup>§</sup> *Institute for Theoretical Physics,  
University of Bern, Sidlerstrasse 5, CH-3012, Bern, Switzerland*<sup>\*\*</sup> *HEPI, Tbilisi State University, 380086 Tbilisi, Georgia*

(Pacs Numbers: 12.39.Ki, 12.60.Rc, 13.30.Eg, 13.30.Hq, 14.20.Lq, 14.20.Mr)

**Abstract**

We analyze strong one-pion and radiative one-photon decays of heavy flavored baryons within a relativistic three-quark model. Employing the same parameters as were used for the description of the semileptonic decays of heavy baryons, we calculate the couplings of one-pion and one-photon transitions of both ground and excited heavy baryon states. We predict the decay rates for all relevant decay modes and compare them with experimental data when available and with the results of other model calculations.

**I. INTRODUCTION**

The last decade has seen significant experimental progress in charm baryon physics. Most of the ground state baryons containing one c-quark have now been established [1]. Their classification in the standard quark model is based on three different spin configurations: the lowest lying configuration has  $J^P = \frac{1}{2}^+$  ( $\Lambda_c$ ,  $\Xi_c$ ) with the two light quarks in the antisymmetric spin 0 configuration, the next higher configuration  $J^P = \frac{1}{2}^+$  ( $\Sigma_c$ ,  $\Xi'_c$ ,  $\Omega_c$ ) and the highest configuration  $J^P = \frac{3}{2}^+$  ( $\Sigma_c^*$ ,  $\Xi_c^*$ ,  $\Omega_c^*$ ) where the two light quarks are in the symmetric spin 1 configuration, coupling down and up to  $\frac{1}{2}^+$  and  $\frac{3}{2}^+$ , respectively, with the heavy quark. Some of their decay modes have been seen and have been used for the determination of their masses (see [1]).

The CLEO Coll. [2] has presented evidence for a pair of excited charm baryons, one decaying into  $\Lambda_c^+ \pi^+$  with a mass difference  $M(\Lambda_c^+ \pi^+) - M(\Lambda_c^+)$  of  $234.5 \pm 1.1 \pm 0.8$  MeV and a width of  $17.9^{+3.8}_{-3.2} \pm 4.0$  MeV, and the other into  $\Lambda_c^+ \pi^-$  with a mass difference  $M(\Lambda_c^+ \pi^-) -$

$M(\Lambda_c^+)$  of  $232 \pm 1.0 \pm 0.8$  MeV and a width of  $13.0_{-3.0}^{+3.7} \pm 4.0$  MeV. The CLEO Coll. interpreted these data as evidence for the  $\Sigma_c^{*++}$  and  $\Sigma_c^{*0}$ , the spin  $\frac{3}{2}^+$  excitations of the  $\Sigma_c$  baryons.

Earlier, the CLEO Coll. [3] has also reported evidence for a pair of excited charmed baryons, one decaying into  $\Xi_c^+ \pi^-$  with a mass difference  $M(\Xi_c^+ \pi^-) - M(\Xi_c^+)$  of  $178.2 \pm 0.5 \pm 1.0$  MeV and a width of  $< 5.5$  MeV, and the other [4] into  $\Xi_c^0 \pi^+$  with a mass difference  $M(\Xi_c^0 \pi^+) - M(\Xi_c^0)$  of  $174.3 \pm 0.5 \pm 1.0$  MeV and a width of  $< 3.1$  MeV. They interpreted these data as evidence for the  $\Xi_c^{*0}$  and  $\Xi_c^{*+}$ , the spin  $\frac{3}{2}^+$  excitations of the  $\Xi_c$  baryons.

Recently, the CLEO Coll. [5] has reported on the observation of two narrow states in the decay modes  $\Xi_c^+ \gamma$  and  $\Xi_c^0 \gamma$ . They have been interpreted as the  $\Xi_c'$  states. The mass differences  $M(\Xi_c^{*+}) - M(\Xi_c^+)$  and  $M(\Xi_c^{*0}) - M(\Xi_c^0)$  have been measured to be  $107.8 \pm 1.7 \pm 2.5$  MeV and  $107.0 \pm 1.4 \pm 2.5$  MeV, respectively. Except for the  $\Omega_c^*$  and some of the isospin partners of the charm baryon ground states most of the ground state charm baryons are now well established.

Three collaborations (ARGUS [6], E687 [7] and CLEO [8]) have seen a doublet of particles decaying into  $\Lambda_c^+ \pi^+ \pi^-$ . They have been interpreted as the lowest lying orbitally excited states of the  $\Lambda_c^+$ :  $\Lambda_{c1}^+(2593)$  with  $J^P = \frac{1}{2}^-$  and  $\Lambda_{c1}^{*+}(2625)$  with  $J^P = \frac{3}{2}^-$ . The PDG average for the decay width of the  $\Lambda_{c1}^+(2593)$  is  $3.6_{-1.3}^{+2.0}$  MeV. The branching fractions into the  $\Lambda_c^+ \pi^+ \pi^-$  and the  $\Sigma_c^{*+}(2455) \pi^-$  and  $\Sigma_c^0(2455) \pi^+$  modes are estimated to be  $\approx 67\%$ ,  $24 \pm 7\%$  and  $18 \pm 7\%$ , respectively. For the decay width of the  $\Lambda_{c1}^+(2625)$  there exists only an upper limit ( $< 1.9$  MeV) and branching ratios [1], [6]- [8].

The CLEO Coll. [9] has reported preliminary evidence for a new charm baryon decaying into  $\Xi_c^+ \pi^+ \pi^-$  via the intermediate  $\Xi_c^{*0}$ -state. The measured mass difference is given by  $M(\Xi_c^+ \pi^+ \pi^-) - M(\Xi_c^+) = 349.4 \pm 0.7 \pm 1.0$  MeV, and its width is  $\Gamma < 2.4$  MeV. This new particle was interpreted as the  $\Xi_{c1}^{*+}$  with  $J^P = \frac{3}{2}^-$ , the charm-strange partner of the  $\Lambda_{c1}^{*+}(2625)$ .

The classification and the decay properties of ground and excited state charm and bottom baryons have been reviewed in [10]. The analysis was based on the heavy quark limit given by the leading order in the  $1/m_Q$ -expansion. In the heavy quark limit the dynamics of the heavy and light quarks decouple leading to a number of model independent relations between various decay modes of the heavy baryons. Further relations between physical observables can be obtained if one assumes additional symmetries for the light quark system. For instance, by using a constituent quark model picture for the light diquark system with an underlying  $SU(2N_f) \otimes O(3)$  symmetry, a number of further relations were derived in [11] for the form factors in semileptonic  $b - c$  transitions.

The subject of this paper mostly concerns the one-pion and one-photon decays of ground state charm baryons as well as those of the lowest-lying p-wave states. We shall also determine the one-photon decays of the orbital excitations of bottom baryons. The analysis of these transitions provides an excellent laboratory for tests of heavy quark symmetry predictions on the one hand and tests of the soft dynamics of the light-side one-pion (photon) diquark transitions on the other hand. In the heavy quark limit the pion and photon are emitted from the light diquark system while the heavy quark is unaffected by the emission process.

Single pion transitions of charm baryons were analyzed before in [10,12] by again using the constituent quark model picture for the light diquark system with its underlying  $SU(2N_f) \otimes O(3)$  symmetry. Using this symmetry one significantly reduces the number of independent

coupling factors [10,12].

A similar constituent quark model approach has been employed in [13] to establish relationships among the coupling constants characterizing the decays of s-wave and p-wave heavy baryons. The results of the work [13] are the same as in [12] since both approaches are based on the same constituent quark model picture.

Light-front (LF) quark model functions with a factorized harmonic-oscillator transverse momentum component and a longitudinal component given by a  $\delta$ -function have been constructed in [14]. They have been employed to calculate the strong couplings for  $\Sigma_c \rightarrow \Lambda_c \pi$ ,  $\Lambda_{c1} \rightarrow \Sigma_c \pi$ , and  $\Lambda_{c1}^* \rightarrow \Sigma_c \pi$  decay modes which correspond to P-wave, S-wave and D-wave transitions, respectively.

The flavor-spin symmetry of the heavy quarks and the spontaneously broken  $SU(3)_L \otimes SU(3)_R$  chiral symmetry of the light quarks were exploited to describe the interactions of heavy mesons and heavy baryons with the  $\pi$ ,  $K$ , and  $\eta$  mesons considered as the Goldstone bosons [15]. This approach contains three free parameters and was applied to strong and semileptonic decays of heavy hadrons. The radiative decays of heavy mesons and heavy baryons were also studied within this formalism in [16]. The two orbital excitations of the  $\Lambda_c$  have been analyzed within this approach which is referred to as the heavy hadron chiral perturbation theory (HHCPT) by Cho [17] (see also [13]). Information on one of the three free parameters of HHCPT in these decays was obtained from the radiative decay  $\Xi_c'^{*0} \rightarrow \Xi_c^0 \gamma$  by Cheng [18]. Pion transitions of the ground states and some excited p-wave states of heavy baryons were studied within HHCPT in [19]. The coupling constants were estimated using the experimental data on the pion decays of strange  $\Lambda$  and  $\Sigma$  baryons treating the  $s$ -quark as static.

The radiative decays of some excited heavy baryon states have been calculated in the so-called bound state picture [20] motivated by the large  $N_c$  limit. It was shown that the  $\Lambda_{c1}(2593) \rightarrow \Lambda_c \gamma$  and  $\Lambda_{c1}^*(2625) \rightarrow \Lambda_c \gamma$  decays are severely suppressed whereas the  $\Lambda_{b1}^*(5900) \rightarrow \Lambda_b \gamma$  mode possibly dominates over the strong decay mode.

Some aspects of the phenomenology of new baryons with charm and strangeness were discussed in [21]. The authors of Ref. [21] estimated the expected width of the excited state  $\Xi_{c1}(\frac{3}{2})^+$  of the  $\Xi_c$  family using the experimental value for the width of the  $\Lambda_{c1}(\frac{1}{2})^+$  within the  $SU(3)$  flavor symmetry limit. Also it was pointed out that one should search for the  $\Omega_{c2}^*$  baryon in the  $\Xi_c K$  decay channel.

The ratio of electric quadrupole (E2) and magnetic dipole (M1) components for the decay  $\Sigma_c^* \rightarrow \Lambda_c \gamma$  has been computed by Savage [22] within the HHCPT approach. The result was that the  $1/m_c$  suppression of the E2 amplitude is compensated for by a small energy denominator arising from the infrared behavior of pion loop graphs in chiral perturbation theory. This leads to a  $E2/M1$  ratio of the order of a few percent depending among others on the  $\Sigma_c^* - \Sigma_c$  spin symmetry breaking mass difference. The corresponding ratio in the bottom baryon sector is smaller by a factor of  $\sim M_c/M_b$ .

The couplings in the HHCPT Lagrangian have been estimated from QCD sum rules in an external axial field [23]. The radiative decays of heavy baryons were studied with the light cone QCD sum rules in the leading order of HQET in [24].

All approaches considered above exploit the symmetry of the heavy quark limit with some additional assumptions on the structure of the light quark system without employing any dynamical scheme for the composite structure of hadrons.

A relativistic quark model of hadrons [25]- [28] has been developed some time ago to describe physical observables in the low-energy domain. The model is based on an effective hadron-quark Lagrangian and the compositeness condition  $Z_H = 0$  where  $Z_H$  is a wave function renormalization constant of the hadron [30]. This approach has been employed to give a unified description of leptonic and semileptonic decays of heavy mesons in [29].

Recently, this model called the Relativistic Three-Quark Model (RTQM) has been applied to calculate physical observables in the decays of heavy baryons [31]- [34]. All results of the RTQM model are expressed through a few model parameters: the masses of the light quarks, the mass differences of the heavy baryon and heavy quark, and the size of the Gaussian distribution of constituents inside the hadron. The exclusive semileptonic and nonleptonic decays of charmed and bottom baryons have been considered within the RTQM [31,32]. Preliminary results for the strong and radiative decays of heavy baryons have been reported in [33,34]. In this paper we extend this application by reporting the simultaneous calculation of a range of one-pion and one-photon transitions between heavy baryons.

Our article is divided into five sections with a single appendix. In Sec. II we give some necessary background material on the RTQM and discuss features of gauging the interaction Lagrangian in this approach. The calculation of the matrix elements of the one-pion and one-photon transitions between heavy baryons is given Sec. III. In Sec. IV we present our numerical results on the heavy baryon observables in their strong and radiative transitions. We compare our results with available experimental data and with the results of some other model approaches. We make some concluding remarks in Sec. V. The Appendix contains a detailed discussion of the gauge invariance of radiative transitions in the RTQM.

## II. RELATIVISTIC THREE-QUARK MODEL

A detailed description of the Relativistic Three-Quark Model can be found in Refs. [28,31]. Here we will only give the necessary background material needed for the description of two-body strong and electromagnetic decays of heavy flavored baryons. We will discuss the interaction Lagrangian describing the coupling of heavy baryons with their constituent quarks and its gauging. We also specify the form of the light and heavy quark propagators.

The Lagrangian describing the coupling of a heavy baryon to its constituent light and heavy quarks considerably simplifies in the heavy quark limit (see [31]). One has

$$\begin{aligned} \mathcal{L}_{BQ}^{\text{int}}(x) &= g_{BQ} \bar{B}_Q(x) \Gamma_1 Q^a(x) \int d\xi_1 \int d\xi_2 F_B(\xi_1^2 + \xi_2^2) \\ &\quad \times q^b(x + 3\xi_1 - \sqrt{3}\xi_2) C \Gamma_2 \lambda_{BQ} q^c(x + 3\xi_1 + \sqrt{3}\xi_2) \varepsilon^{abc} + \text{h.c.} \\ F_B(\xi_1^2 + \xi_2^2) &= \int \frac{d^4 k_1}{(2\pi)^4} \int \frac{d^4 k_2}{(2\pi)^4} e^{ik_1 \xi_1 + ik_2 \xi_2} \tilde{F}_B \left\{ \frac{[k_1^2 + k_2^2]}{\Lambda_B^2} \right\} \end{aligned} \quad (1)$$

The interaction Lagrangian of the pion with its constituent light quarks is given by

$$\mathcal{L}_\pi^{\text{int}}(x) = \frac{ig_\pi}{\sqrt{2}} \vec{\pi}(x) \int d\xi F_\pi(\xi^2) \bar{q}(x + \xi/2) \gamma^5 \vec{\lambda}_\pi q(x - \xi/2) \quad (2)$$

where

$$F_\pi(\xi^2) = \int \frac{d^4 k}{(2\pi)^4} e^{ik\xi} \tilde{F}_\pi \left\{ \frac{k^2}{\Lambda_\pi^2} \right\}$$

Here  $\Gamma_i$  and  $\lambda_{B_Q}$  are spinor and flavor matrices which define the quantum numbers of the relevant three-quark currents. They are listed in Table I. The square brackets [...] and curly brackets {...} denote antisymmetric and symmetric flavor and spin combinations of the light degrees of freedom<sup>1</sup>. The coupling strength of the respective hadrons with their constituent quarks are denoted by the coupling constants  $g_{B_Q}$  and  $g_\pi$ . The parameters  $\Lambda_B$  and  $\Lambda_\pi$  define the size of the distributions of light quarks inside the heavy baryon and pion, respectively. The baryon parameter  $\Lambda_B$  is chosen to be the same for charm and bottom baryons to provide the correct normalization of the baryonic Isgur-Wise function in the heavy quark limit [31].

The gauging of the nonlocal interaction Lagrangian Eq.(2) can be done by using a path-independent formalism based on the path-independent definition [35] of the derivative of the path integral. The details may be found in [36] and also in [28] where this formalism was employed to calculate the nucleon electromagnetic form factors in the quark model in a gauge invariant way. In order to make the Lagrangian Eq.(1) gauge invariant in the presence of an electromagnetic field  $A_\mu(x)$  the time-ordered P-exponent

$$P \exp \left\{ ieQ \int_x^y dz_\mu A^\mu(z) \right\} \quad (3)$$

( $Q = \text{diag}\{2/3, -1/3, -1/3\}$  is the charge matrix) is attached to each light quark field  $q(y)$ . We then have

$$\begin{aligned} \mathcal{L}_{B_Q}^{\text{int,e.m.}}(x) &= g_{B_Q} \bar{B}_Q(x) \Gamma_1 Q^a(x) \int d^4 \xi_1 \int d^4 \xi_2 F_B(\xi_1^2 + \xi_2^2) \\ &\times \exp(ieQ \int_x^{x+3\xi_1-\sqrt{3}\xi_2} dz_\mu A^\mu(z)) q^b(x+3\xi_1-\sqrt{3}\xi_2) C \Gamma_2 \lambda_{B_Q} \\ &\times \exp(ieQ \int_x^{x+3\xi_1+\sqrt{3}\xi_2} dz_\mu A^\mu(z)) q^c(x+3\xi_1+\sqrt{3}\xi_2) \varepsilon^{abc} + \text{h.c.} \end{aligned} \quad (4)$$

The Lagrangian Eq. (4) generates nonlocal vertices which involve the heavy baryons, photons and the light and heavy quarks. The gauge formalism of Mandelstam is based on the definition of the derivative of the path integral

$$I(y, x, P) = \int_x^y dz_\mu A^\mu(z) \quad (5)$$

---

<sup>1</sup>We use the following notation for excited heavy  $P$ -wave baryons:

i)  $\Lambda_{c1;S}$ ,  $\Lambda_{c1;S}^*$ ,  $\Sigma_{c0;S}$  and  $\Xi_{c1;S}^*$  are symmetric under the exchange of the momenta of the two light quarks (called  $K$ -states in [10–12]); ii)  $\Sigma_{c1;A}$  and  $\Sigma_{c1;A}^*$  are antisymmetric under the exchange of the momenta of the two light quarks (called  $k$ -states in [10–12]).

where  $P$  is the path taken from  $x$  to  $y$ . When calculating Feynman diagrams the derivative of  $I(y, x, P)$  is defined such that

$$\frac{\partial}{\partial y^\mu} I(y, x, P) = A_\mu(y).$$

This means that the field  $A_\mu(y)$  does not depend on the path used in the definition of the line integral. The Mandelstam prescription makes all matrix elements involving a photon gauge-invariant and path-independent.

The free quark Lagrangian and the interaction Lagrangian for transitions involving the orbital excited states (P-states, etc.) are gauged by the standard minimal substitution, i.e. for the derivative coupling appearing in the  $P$ -states one has to replace  $\partial_\mu \rightarrow \partial_\mu + ieA_\mu$ .

Now we discuss the implementation of gauge invariance in the one-photon transitions of heavy baryons. There are several relevant diagrams: i) the triangle diagrams in Fig. 2a and 2b with a photon emitted by the heavy and light quark, respectively ii) the contact interaction-type diagrams in Fig. 3 with a photon emitted by one of the two nonlocal baryon-quark vertices and iii) the pole diagrams in Fig. 4 with a photon emitted by one of the two heavy baryons.

The contributions coming from the triangle diagram in Fig. 2a and the pole diagrams in Fig. 4 are nonleading in  $1/m_Q$  and vanish in the heavy quark limit. The contact interaction-type diagrams in Fig. 3 are important to reproduce the Ward-Takahashi identities for the connected Green functions (see, for example, Ref. [28]). Their contributions to the matrix element of the one-photon transitions of ground state charm baryons are nonleading in the heavy mass expansion, at least when the photon is on its mass shell ( $q^2 = 0$ ). However, they contribute to the matrix elements of one-photon transitions of the orbitally excited charm baryon states  $B_{c1} \rightarrow B_c \gamma$  and  $B_{c1}^* \rightarrow B_c \gamma$  where  $B_c = \Lambda_c$  or  $\Xi_c$ . Formally the contact interaction type contributions in this case are of the order  $O(qv) \approx O(0)$  ( $qv = (m_i^2 - m_f^2)/(2m_i) \approx 0$ ) and one would naively assume that they vanish in the heavy quark limit. However, contrary to the ground state transitions, the excited state transitions  $B_{c1} \rightarrow B_c \gamma$  and  $B_{c1}^* \rightarrow B_c \gamma$  are of the same order  $Q(qv)$  and thus the contact interaction-type contribution must be kept in this case. In the Appendix we provide a detailed discussion of the gauge-invariance structure of the matrix elements for one-photon transitions of excited charm baryons<sup>2</sup>.

For radiative transitions involving P-wave states there are additional contact interaction-type diagrams which contribute to the leading order in the heavy quark expansion. They result from the minimal substitution prescription for the derivatives acting on the excited heavy baryon fields in the heavy baryon-three-quark interaction Lagrangian (1). In the following we will refer to such diagrams as "local contact" diagrams in order to distinguish them from the contact diagrams generated by the gauging of the nonlocal heavy baryon-three-quark vertex ("nonlocal contact" diagrams).

---

<sup>2</sup>In our previous analysis of we neglected the contact interaction-type diagrams of the  $P$ -wave heavy baryon transitions [34]. Their contribution to the invariant matrix element is very small of order 3-4%. We demonstrate in the Appendix that the contact interaction-type contribution is needed to reproduce the correct gauge invariance structure of the photon transitions.

Thus, in the heavy quark limit the radiative decay of a ground state heavy baryon is described by the solely triangle diagram in Fig. 2b with the photon emitted by the light quark whereas there are additional contributions coming from both the “nonlocal contact” in Fig. 3 and “local contact” in Fig. 4 diagrams for the radiative decays of heavy excited baryon states. For the one-pion transitions one only needs the only triangle diagram depicted in Fig. 1.

Let us now specify our model parameters. For the light quark propagator with a constituent mass  $m_q$  we shall use the standard form of the free fermion propagator

$$S_q(k) = \frac{1}{m_q - \not{k}}. \quad (6)$$

For the heavy quark propagator we shall use the leading term  $S_v(k, \bar{\Lambda}_{\{q_1 q_2\}})$  in the inverse mass expansion of the free fermion propagator:

$$\begin{aligned} S_Q(p+k) &= \frac{1}{m_Q - (\not{p} + \not{k})} = S_v(k, \bar{\Lambda}_{\{q_1 q_2\}}) + O\left(\frac{1}{m_Q}\right), \\ S_v(k, \bar{\Lambda}_{\{q_1 q_2\}}) &= -\frac{1 + \not{v}}{2(vk + \bar{\Lambda}_{\{q_1 q_2\}})}. \end{aligned} \quad (7)$$

where we introduce the mass difference parameter  $\bar{\Lambda}_{\{q_1 q_2\}} = M_{\{Q q_1 q_2\}} - m_Q$  which is the difference between the heavy baryon mass  $M_{\{Q q_1 q_2\}} \equiv M_{B_Q}$  and the heavy quark mass  $m_Q$ . The four-velocity of the heavy quark is denoted by  $v$  as usual. We shall neglect a possible mass difference between the constituent  $u$ - and  $d$ -quark and thus take  $\bar{\Lambda} := \bar{\Lambda}_{uu} = \bar{\Lambda}_{ud} = \bar{\Lambda}_{dd}$ ,  $\bar{\Lambda}_s := \bar{\Lambda}_{us} = \bar{\Lambda}_{ds}$  meaning that there are altogether three independent mass difference parameters:  $\bar{\Lambda}$ ,  $\bar{\Lambda}_s$ , and  $\bar{\Lambda}_{ss}$ .

The vertex functions  $F_B$  and  $F_\pi$  are arbitrary functions except that they should fall off sufficiently fast in the ultraviolet region to render the Feynman diagrams ultraviolet finite. In principle, their functional forms are calculable from the solutions of the Bethe-Salpeter equations for the baryon and pion bound states. For example, in [37] semileptonic meson transitions have been analyzed using the heavy-quark limit of the Dyson-Schwinger equation. The results were found to be quite insensitive to the details of the functional form of the heavy-meson Bethe-Salpeter amplitude. We will use this observation as a guiding principle and choose simple Gaussian forms for the vertices  $F_B$  and  $F_\pi$ . Their Fourier transforms read

$$\tilde{F}_B(k_1^2 + k_2^2) = \exp\left(\frac{k_1^2 + k_2^2}{\Lambda_B^2}\right), \quad \tilde{F}_\pi(k^2) = \exp\left(\frac{k^2}{\Lambda_\pi^2}\right). \quad (8)$$

where  $\Lambda_B$  and  $\Lambda_\pi$  characterize the size of the distributions of the light quarks inside a baryon and pion, respectively.

The coupling constants  $g_{B_Q}$  and  $g_\pi$  in Eqs. (1) and (2) are calculated from *the compositeness condition* (see, ref. [25,30]), which means that the renormalization constant of the hadron wave function is set equal to zero:  $Z_{B_Q} = 1 - g_{B_Q}^2 \Sigma'_{B_Q}(M_{B_Q}) = 0$  where  $\Sigma_{B_Q}$  is a baryon mass operator, and similarly for the pion  $Z_\pi = 1 - g_\pi^2 \Pi'_\pi(m_\pi^2) = 0$  where  $\Pi_\pi$  is a pion mass operator.

A drawback of our approach is the lack of confinement. To avoid the appearance of unphysical imaginary parts in the Feynman diagrams, we shall require that  $M_{B_Q} < m_Q +$

$m_{q_1} + m_{q_2}$  which implies that the mass difference parameter  $\bar{\Lambda}_{q_1 q_2}$  is bounded from above by the requirement  $\bar{\Lambda}_{q_1 q_2} < m_{q_1} + m_{q_2}$ .

As mentioned before the masses of the  $u$  and the  $d$  quarks are set equal ( $m_u = m_d = m_q$ ). The value of  $m_q$  is determined from an analysis of nucleon data:  $m_q=420$  MeV [28]. The pion Gaussian size parameter  $\Lambda_\pi = 1$  GeV is fixed from the description of low-energy pion observables (the coupling constants  $f_\pi$  and  $g_{\pi\gamma\gamma}$ , and the electromagnetic radii and form factors of the transitions  $\pi \rightarrow \pi\gamma$  and  $\pi \rightarrow \gamma\gamma^*$ ) [26]- [27]. The parameters  $\Lambda_B$ ,  $m_s$ ,  $\bar{\Lambda}$  are taken from an analysis of the  $\Lambda_c^+ \rightarrow \Lambda^0 + e^+ + \nu_e$  decay data. A good description of the present average value of the branching ratio  $B(\Lambda_c^+ \rightarrow \Lambda e^+ \nu_e) = 2.2$  % can be achieved using the following values of the parameters  $\Lambda_B$ ,  $m_s$  and  $\bar{\Lambda}$ :  $\Lambda_B=1.8$  GeV,  $m_s=570$  MeV and  $\bar{\Lambda}=600$  MeV. The values of the parameters  $\bar{\Lambda}_s$  and  $\bar{\Lambda}_{ss}$  are determined from the heuristic relations  $\bar{\Lambda}_s = \bar{\Lambda} + (m_s - m)$  and  $\bar{\Lambda}_{ss} = \bar{\Lambda} + 2(m_s - m)$ , which give  $\bar{\Lambda}_s = 750$  MeV and  $\bar{\Lambda}_{ss} = 900$  MeV. We mention that, using the same values of  $\Lambda_{B_Q}=1.8$  GeV and  $\bar{\Lambda}=600$  MeV, one obtains a width of  $5.4 \times 10^{10} s^{-1}$  and a value of  $\rho^2 = 1.4$  for the slope of the Isgur-Wise function in the decay  $\Lambda_b^0 \rightarrow \Lambda_c^+ e^- \bar{\nu}_e$  [33]. Finally, the mass values of the charm baryon states including current experimental errors are listed in TABLE I [1,5]. For the pion masses we take  $m_{\pi^\pm} = 139.6$  MeV and  $m_{\pi^0} = 135$  MeV [1].

All dimensional parameters entering the Feynman diagrams are expressed in units of  $\Lambda_B$ . The integrals are calculated in the Euclidean region both for internal and external momenta. The final results are obtained by analytic continuation of the external momenta to the physical region after the internal momenta have been integrated out.

### III. MATRIX ELEMENTS OF ONE-PION AND ONE-PHOTON TRANSITIONS

We begin our discussion with the one-pion and one-photon transitions of the ground state baryons. As discussed in Sec. II in the heavy quark limit they are described by the triangle two-loop diagrams Fig. 1 and Fig. 2b.

The contribution of the triangle diagram (Fig. 1 and Fig. 2b) to the matrix element of the one-pion (one-photon) transition  $B_Q^i(p) \rightarrow B_Q^f(p') + X(q)$  has the following form in the heavy quark limit

$$M_{inv,\Delta}^X(B_Q^i \rightarrow B_Q^f X) = g_X g_{\text{eff}}^i g_{\text{eff}}^f \cdot \bar{u}(v') \Gamma_1^f \frac{(1 + \not{q})}{2} \Gamma_1^i u(v) \cdot I_{q_1 q_2, \Delta}^{if}(v, q) \quad (9)$$

where the symbol  $X$  denotes a pion or a photon in the final state, i.e.  $X = \pi$  or  $\gamma$  and  $g_X = g_\pi/\sqrt{2}$  (pion-quark-antiquark coupling) or  $e$  (electron charge);  $g_{\text{eff}} = g_{B_Q} \Lambda_B^2/\sqrt{6}/(8\pi^2)$ .  $I_{q_1 q_2, \Delta}^{if}(v, q)$  is a two-loop quark integral the form of which depends on whether one is computing pion or photon transitions. For the pion one has

$$I_{q_1 q_2, \Delta}^{if}(v, q)|_{X=\pi} = \int \frac{d^4 k_1}{\pi^2 i} \int \frac{d^4 k_2}{4\pi^2 i} \frac{\tilde{F}_B(k_1, k_2, q) \tilde{F}_B(k_1, k_2, 0)}{[-k_1 v - \bar{\Lambda}_{q_1 q_2}]} \Pi_{q_1 q_2, \Delta}^\pi(k_1, k_2, q) \quad (10)$$

$$\tilde{F}_B(k_1, k_2, q) \equiv \tilde{F}_B \left\{ -6 \left[ (k_1 + q)^2 + (k_2 - q)^2 + (k_1 + k_2)^2 \right] \right\}$$

Here  $\Pi_{q_1 q_2, \Delta}^\pi(k_1, k_2, q)$  is the structure integral corresponding to the light quark loop:



$$\Pi_{q_1 q_2, \Delta}^\pi(k_1, k_2, q) = C_{\text{flavor}} \tilde{F}_\pi \left\{ - \left( k_2 - \frac{q}{2} \right)^2 \right\} \text{tr} \left[ \Gamma_2^i S_{q_2}(k_1 + k_2) \Gamma_2^f S_{q_1}(k_2 - q) \gamma^5 S_{q_1}(k_2) \right] \quad (11)$$

where  $C_{\text{flavor}} = \text{tr}[\lambda_\pi \lambda_{B^i} \lambda_{B^f}]$  is a trace of flavor matrices and  $\Gamma_{1(2)}^i$  and  $\Gamma_{1(2)}^f$  are the Dirac matrices of the initial and the final baryons, respectively.

For the photon transition one has

$$I_{q_1 q_2, \Delta}^{if}(v, q)|_{X=\gamma} = \varepsilon_\mu^*(q) \int \frac{d^4 k_1}{\pi^2 i} \int \frac{d^4 k_2}{4\pi^2 i} \frac{\tilde{F}_B(k_1, k_2, q) \tilde{F}_B(k_1, k_2, 0)}{[-k_1 v - \bar{\Lambda}_{q_1 q_2}]} \Pi_{q_1 q_2, \Delta}^{\gamma; \mu}(k_1, k_2, q) \quad (12)$$

$$\tilde{F}_B(k_1, k_2, q) \equiv \tilde{F}_B \left\{ -6 \left[ (k_1 + q)^2 + (k_2 - q)^2 + (k_1 + k_2)^2 \right] \right\}$$

$$\begin{aligned} \Pi_{q_1 q_2, \Delta}^{\gamma; \mu}(k_1, k_2, q) &= Q_{q_2 q_2} \text{tr} \left[ \Gamma_2^i S_{q_1}(k_1 + k_2) \Gamma_2^f S_{q_2}(k_2 - q) \gamma^\mu S_{q_2}(k_2) \right] \\ &\quad - Q_{q_1 q_1} \text{tr} \left[ \Gamma_2^f S_{q_2}(-k_1 - k_2) \Gamma_2^i S_{q_1}(-k_2) \gamma^\mu S_{q_1}(-k_2 + q) \right] \end{aligned} \quad (13)$$

where  $\varepsilon_\mu^*(q)$  is the polarization vector of the photon.

Radiative transitions of excited heavy baryon states involve additional contributions from the "local contact" and "nonlocal contact" diagrams. In our recent analysis [34] we have neglected the "nonlocal contact" diagrams because their contribution to the corresponding invariant matrix elements is quite small (of order 3-4%). Here we present a complete analysis of radiative transitions of heavy baryons by taking into account all possible diagrams contributing to these processes in the heavy quark limit as is necessary to obtain a gauge invariant result. In the heavy quark limit the contributions of the "local contact" diagrams (lcd) and "nonlocal contact" diagrams (ncd) to the matrix element of the excited heavy baryon transition  $B_{Q1}^i(p) \rightarrow B_Q^f(p') + \gamma$  simplify to

$$M_{\text{inv, lcd}}^\gamma(B_{Q1}^i \rightarrow B_Q^f \gamma) = e g_{\text{eff}}^i g_{\text{eff}}^f \cdot \bar{u}(v') \Gamma_1^f \frac{(1 + \not{v}')}{2} \Gamma_1^i u_\nu(v) \cdot I_{q_1 q_2, \text{lcd}}^{if, \nu}(v, q) \quad (14)$$

$$I_{q_1 q_2, \text{lcd}}^{if, \nu}(v, q) = -\varepsilon_\nu^*(q) \int \frac{d^4 k_1}{\pi^2 i} \int \frac{d^4 k_2}{4\pi^2 i} \frac{\tilde{F}_B(k_1, k_2, 0) \tilde{F}_B(k_1, k_2, -q)}{[-k_1 v' - \bar{\Lambda}_{q_1 q_2}]} \Pi_{q_1 q_2}^\gamma(k_1, k_2)$$

where

$$\Pi_{q_1 q_2}^\gamma(k_1, k_2) = Q_{q_2 q_2} \text{tr} \left[ \Gamma_2^i S_{q_2}(k_1 + k_2) \Gamma_2^f S_{q_2}(k_2) \right] + Q_{q_1 q_1} \text{tr} \left[ \Gamma_2^f S_{q_2}(k_1 + k_2) \Gamma_2^i S_{q_1}(k_2) \right]$$

and

$$\begin{aligned} M_{\text{inv, ncd}}^\gamma(B_{Q1}^i \rightarrow B_Q^f \gamma) &= e g_{\text{eff}}^i g_{\text{eff}}^f \cdot \bar{u}(v') \Gamma_1^f \left[ \frac{(1 + \not{v}')}{2} I_{q_1 q_2, \text{ncd}}^{if, \nu; L}(v, q) \right. \\ &\quad \left. + \frac{(1 + \not{v}')}{2} I_{q_1 q_2, \text{ncd}}^{if, \nu; R}(v, q) \right] \Gamma_1^i u_\nu(v) \end{aligned} \quad (15)$$

$$\begin{aligned}
I_{q_1 q_2, \text{ncd}}^{if, \nu; L}(v, q) &= \varepsilon_\mu^*(q) \int \frac{d^4 k_1}{\pi^2 i} \int \frac{d^4 k_2}{4\pi^2 i} (k_1 - k_2 + q)^\mu k_1^\nu \frac{\tilde{F}_B(k_1, k_2, 0)}{[-k_1 v - \Lambda_{q_1 q_2}]} \\
&\times \frac{\tilde{F}_B(k_1, k_2, 0) - \tilde{F}_B(k_1, k_2, q)}{(k_1 - k_2)q + q^2} \Pi_{q_1 q_2}^\gamma(k_1, k_2)
\end{aligned} \tag{16}$$

$$\begin{aligned}
I_{q_1 q_2, \text{ncd}}^{if, \nu; R}(v, q) &= \varepsilon_\mu^*(q) \int \frac{d^4 k_1}{\pi^2 i} \int \frac{d^4 k_2}{4\pi^2 i} (k_1 - k_2 - q)^\mu k_1^\nu \frac{\tilde{F}_B(k_1, k_2, 0)}{[-k_1 v' - \Lambda_{q_1 q_2}]} \\
&\times \frac{\tilde{F}_B(k_1, k_2, 0) - \tilde{F}_B(k_1, k_2, -q)}{(k_2 - k_1)q + q^2} \Pi_{q_1 q_2}^\gamma(k_1, k_2)
\end{aligned} \tag{17}$$

As an illustration of our calculational procedure we evaluate a typical integral corresponding to a one-photon transition (the same integral for the one-pion transition can be found in Ref. [33])

$$R_{q_1 q_2}^{if; \mu}(v, q) = \int \frac{d^4 k_1}{\pi^2 i} \int \frac{d^4 k_2}{\pi^2 i} \frac{\tilde{F}_B(k_1, k_2, q) \tilde{F}_B(k_1, k_2, 0)}{[-k_1 v - \Lambda_{q_1 q_2}]} \text{tr}[\Gamma_2^i S_{q_2}(k_1 + k_2) \Gamma_2^f S_{q_1}(k_2 - q) \gamma^\mu S_{q_1}(k_2)]$$

We have

$$\begin{aligned}
R_{q_1 q_2}^{if; \mu}(v, q) &= \int_0^\infty ds_1 \tilde{F}_B^L(6s_1) \int_0^\infty ds_2 \tilde{F}_B^L(6s_2) e^{2s_2 q^2} \int_0^\infty d^4 \alpha e^{\alpha_3 \bar{\Lambda} - (\alpha_1 + \alpha_4) m_{q_1}^2 - \alpha_2 m_{q_2}^2} \\
&\times \text{tr} \left[ \Gamma_2^i \left( m_{q_2} - \frac{\not{\partial}_1 + \not{\partial}_2}{2} \right) \Gamma_2^f \left( m_{q_1} - \frac{\not{\partial}_2}{2} - \not{q} \right) \gamma^\mu \left( m_{q_1} - \frac{\not{\partial}_2}{2} \right) \right] \int \frac{d^4 k_1}{\pi^2 i} \int \frac{d^4 k_2}{\pi^2 i} e^{k A k - 2k B}
\end{aligned}$$

where the matrices A and B are defined by

$$A_{ij} = \begin{pmatrix} 2(s_1 + s_2) + \alpha_2 & s_1 + s_2 + \alpha_2 \\ s_1 + s_2 + \alpha_2 & 2(s_1 + s_2) + \alpha_1 + \alpha_2 + \alpha_4 \end{pmatrix}$$

$$B_i = \begin{pmatrix} -s_2 q - \alpha_3 v/2 \\ (s_2 + \alpha_1) q \end{pmatrix}$$

The integration over  $k_1$  and  $k_2$  results in

$$\begin{aligned}
R_{q_1 q_2}^{if; \mu}(v, q) &= \int_0^\infty ds_1 \tilde{F}_B^L(6s_1) \int_0^\infty ds_2 \tilde{F}_B^L(6s_2) e^{2s_2 q^2} \int_0^\infty d^3 \alpha e^{\alpha_3 \bar{\Lambda} - (\alpha_1 + \alpha_4) m_{q_1}^2 - \alpha_2 m_{q_2}^2} \\
&\times \text{tr} \left[ \Gamma_2^i \left( m_{q_2} - \frac{\not{\partial}_1 + \not{\partial}_2}{2} \right) \Gamma_2^f \left( m_{q_1} - \frac{\not{\partial}_2}{2} - \not{q} \right) \gamma^\mu \left( m_{q_1} - \frac{\not{\partial}_2}{2} \right) \right] \frac{e^{-B A^{-1} B}}{|A|^2}
\end{aligned}$$

Let us, as an example, choose  $\Gamma_2^i = \gamma^\nu$  and  $\Gamma_2^f = \gamma^5$ . In the limit  $qv = (m_i^2 - m_f^2)/(2m_i) \approx 0$  where  $m_i$  and  $m_f$  are the masses of the initial and the final baryons, respectively, we find

$$R_{q_1 q_2}^{\text{VP}; \mu\nu}(v, q) = 4i \varepsilon^{\mu\nu\alpha\beta} q^\alpha v^\beta \cdot \int_0^\infty \frac{d^3 \alpha \alpha_1 \alpha_3}{2|A|^2} \tilde{F}_B^2(6z) \{m_{q_1} (A_{11}^{-1} + A_{12}^{-1}) - m_{q_2} A_{12}^{-1}\}$$

$$A_{ij} = \begin{pmatrix} 2 + \alpha_2 & 1 + \alpha_2 \\ 1 + \alpha_2 & 2 + \alpha_1 + \alpha_2 \end{pmatrix}, \quad A_{ij}^{-1} = \frac{1}{|A|} \begin{pmatrix} 2 + \alpha_1 + \alpha_2 & -(1 + \alpha_2) \\ -(1 + \alpha_2) & 2 + \alpha_2 \end{pmatrix}$$

The evaluation of the other remaining matrix elements proceeds along similar lines.

In the case of one-pion transitions the general expansion of the transition matrix elements  $M_{\text{inv}}^\pi(B_Q^i \rightarrow B_Q^f \pi)$  into a minimal set of covariants reads

$$\begin{aligned} & \text{One-pion transitions} \tag{18} \\ M_{\text{inv}}^\pi(\Sigma_c \rightarrow \Lambda_c \pi) &= \frac{1}{\sqrt{3}} g_{\Sigma_c \Lambda_c \pi} I_1 \bar{u}(v') \not{q} \gamma_5 u(v) \quad \underline{\text{p-wave transition}} \\ M_{\text{inv}}^\pi(\Sigma_c^* \rightarrow \Lambda_c \pi) &= g_{\Sigma_c^* \Lambda_c \pi} I_1 \bar{u}(v') q_\mu u^\mu(v) \quad \underline{\text{p-wave transition}} \\ M_{\text{inv}}^\pi(\Lambda_{c1;S} \rightarrow \Sigma_c \pi) &= f_{\Lambda_{c1;S} \Sigma_c \pi} I_3 \bar{u}(v') u(v) \quad \underline{\text{s-wave transition}} \\ M_{\text{inv}}^\pi(\Lambda_{c1;S}^* \rightarrow \Sigma_c \pi) &= \frac{1}{\sqrt{3}} f_{\Lambda_{c1;S}^* \Sigma_c \pi} I_3 \bar{u}(v') \gamma_5 \not{q} q_\mu u^\mu(v) \quad \underline{\text{d-wave transition}} \end{aligned}$$

where the  $I_1$  and  $I_3$  are the flavor factors which are directly connected to the flavor coefficients  $C_{\text{flavor}}$  (see Eq. (11)) via the relations  $I_i = f_i \cdot C_{\text{flavor}}$ ,  $i = 1$  or  $3$ . The sets of  $I_i$  and  $f_i$  are given in Table II. We have also indicated the orbital angular momentum of the pion in Eq. (18).

For the one-photon transitions one similarly has

$$\begin{aligned} & \text{One-photon transitions} \tag{19} \\ M_{\text{inv}}^\gamma(\Sigma_c \rightarrow \Lambda_c \gamma) &= \frac{2i}{\sqrt{3}} f_{\Sigma_c \Lambda_c \gamma} \bar{u}(v') \not{q} \not{\epsilon}^*(q) u(v) \quad \underline{\text{M1 transition}} \\ M_{\text{inv}}^\gamma(\Sigma_c^* \rightarrow \Lambda_c \gamma) &= 2 f_{\Sigma_c^* \Lambda_c \gamma} \bar{u}(v') \epsilon(\mu \epsilon^* v q) u^\mu(v) \quad \underline{\text{M1 transition}} \\ M_{\text{inv}}^\gamma(\Sigma_c^* \rightarrow \Sigma_c \gamma) &= 2i f_{\Sigma_c^* \Sigma_c \gamma} \bar{u}(v') \frac{\gamma^\mu \gamma^5}{\sqrt{3}} u^\nu(v) (q_\mu \epsilon_\nu^*(q) - q_\nu \epsilon_\mu^*(q)) \quad \underline{\text{M1 transition}} \\ M_{\text{inv}}^\gamma(\Lambda_{c1;S} \rightarrow \Lambda_c \gamma) &= \bar{u}(v') F_{\Lambda_{c1;S} \Lambda_c \gamma} [g^{\mu\nu} v q - v^\mu q^\nu] \frac{\gamma^\nu \gamma^5}{\sqrt{3}} u(v) \epsilon_\mu^*(q) \quad \underline{\text{E1 transition}} \\ M_{\text{inv}}^\gamma(\Lambda_{c1;S}^* \rightarrow \Lambda_c \gamma) &= \bar{u}(v') F_{\Lambda_{c1;S}^* \Lambda_c \gamma}^* [g^{\mu\nu} v q - v^\mu q^\nu] u^\nu(v) \epsilon_\mu^*(q) \quad \underline{\text{E1 transition}} \end{aligned}$$

where the couplings are manifestly gauge invariant. In writing down the one-photon coupling structure in Eq. (19) we have omitted the E2 coupling in the  $\Sigma_c^* \rightarrow \Lambda_c \gamma$  transition and the M2 coupling in the  $\Lambda_{c1;S}^* \rightarrow \Lambda_c \gamma$  transitions as predicted by heavy quark symmetry [10]. Since heavy quark symmetry is manifest in our model calculation the coupling structure (19) is sufficient for our purposes. In the heavy quark limit the coupling constants in Eqs. (18) and (19) become flavor independent. Also some of the above coupling constants become related in the heavy quark limit. The relations read [10,15,17]

$$g_{\Sigma_c \Lambda_c \pi} = g_{\Sigma_c^* \Lambda_c \pi} = g, \quad f_{\Sigma_c \Lambda_c \gamma} = f_{\Sigma_c^* \Lambda_c \gamma} = f, \quad F_{\Lambda_{c1;S} \Lambda_c \gamma} = F_{\Lambda_{c1;S}^* \Lambda_c \gamma} = F \tag{20}$$

Returning to our model calculation the coupling constant  $f$  can be represented as

$$f = (\mu_1 - \mu_2) \frac{R_{\Sigma_Q \Lambda_Q \gamma}}{\sqrt{R_{\Lambda_Q}} \sqrt{R_{\Sigma_Q}}} \tag{21}$$

$$R_{\Sigma_Q \Lambda_Q \gamma} = \frac{1}{4} \int_0^\infty d^3 \alpha \alpha_3 (\alpha_1 + \alpha_2) \tilde{F}_B^2(6z) \frac{A_{11}^{-1}}{|A|^2}$$

$$R_{B_Q} = \int_0^\infty d^3 \alpha \alpha_3 \frac{\tilde{F}_B^2(6z)}{|A|^2} \left\{ 1 + d_{B_Q} \frac{\alpha_3}{m_q^2} \frac{\partial z}{\partial \alpha_3} - \frac{\alpha_3^2}{4m_q^2} A_{12}^{-1} (A_{11}^{-1} + A_{12}^{-1}) \right\}$$

where  $\mu_i = e_i/(2m_q)$  is the magnetic moment of the  $i$ -th light quark. Here

$$z = \frac{\alpha_3^2}{4} A_{11}^{-1} + m_q^2 (\alpha_1 + \alpha_2) - \bar{\Lambda} \alpha_3, \quad d_{B_Q} = \begin{cases} 1 & \text{for } B_Q = \Lambda_Q \\ \frac{1}{2} & \text{for } B_Q = \Sigma_Q \end{cases}$$

The calculation of the other coupling factors proceeds along similar lines. In addition to the relations (20) there is the identity between  $f_{\Sigma_c^* \Lambda_c \gamma}$  and  $f_{\Sigma_c^* \Sigma_c \gamma}$  couplings obtained in the constituent quark model [11,12]:

$$f_{\Sigma_c^* \Lambda_c \gamma} / f_{\Sigma_c^* \Sigma_c \gamma} = (\mu_1 - \mu_2) / (\mu_1 + \mu_2) = 3$$

In our model the light diquark current in  $\Sigma_c$ -baryon is different than that in  $\Lambda_c$ -baryon (see TABLE I). However numerically the latter relation are reproduced with an accuracy 1%.

One can then go on and calculate the one-pion and one-photon decay rates using the general formula

$$\Gamma(B_Q^i \rightarrow B_Q^f X) = \frac{1}{2J+1} \frac{|\vec{q}|}{8\pi M_{B_Q}^2} \sum_{spins} |M_{inv}^\pi(B_Q^i \rightarrow B_Q^f X)|^2 \quad (22)$$

where  $|\vec{q}|$  is the pion (photon) momentum in the rest frame of the decaying baryon. In terms of the coupling constants (20) one obtains

$$\begin{aligned} \Gamma(\Sigma_c \rightarrow \Lambda_c \pi) &= g^2 I_1^2 \frac{|\vec{q}|^3}{6\pi} \frac{M_{\Lambda_c}}{M_{\Sigma_c}} \\ \Gamma(\Sigma_c^* \rightarrow \Lambda_c \pi) &= g^2 I_1^2 \frac{|\vec{q}|^3}{6\pi} \frac{M_{\Lambda_c}}{M_{\Sigma_c^*}} \\ \Gamma(\Lambda_{c1;S} \rightarrow \Sigma_c \pi) &= f_{\Lambda_{c1;S} \Sigma_c \pi}^2 I_3^2 \frac{|\vec{q}|}{2\pi} \frac{M_{\Sigma_c}}{M_{\Lambda_{c1;S}}} \\ \Gamma(\Lambda_{c1;S}^* \rightarrow \Sigma_c \pi) &= f_{\Lambda_{c1;S}^* \Sigma_c \pi}^2 I_3^2 \frac{|\vec{q}|^5}{18\pi} \frac{M_{\Sigma_c}}{M_{\Lambda_{c1;S}^*}} \\ \Gamma(\Sigma_c \rightarrow \Lambda_c \gamma) &= \frac{4}{3\pi} f^2 |\vec{q}|^3 \frac{M_{\Lambda_c}}{M_{\Sigma_c}} \\ \Gamma(\Sigma_c^* \rightarrow \Lambda_c \gamma) &= \frac{4}{3\pi} f^2 |\vec{q}|^3 \frac{M_{\Lambda_c}}{M_{\Sigma_c^*}} \\ \Gamma(\Sigma_c^* \rightarrow \Sigma_c \gamma) &= \frac{4}{9\pi} f_{\Sigma_c^* \Sigma_c \gamma}^2 |\vec{q}|^3 \frac{M_{\Sigma_c}}{M_{\Sigma_c^*}} \\ \Gamma(\Lambda_{c1;S} \rightarrow \Lambda_c \gamma) &= \frac{1}{3\pi} F^2 |\vec{q}|^3 \frac{M_{\Lambda_c}}{M_{\Lambda_{c1;S}}} \\ \Gamma(\Lambda_{c1;S}^* \rightarrow \Lambda_c \gamma) &= \frac{1}{3\pi} F^2 |\vec{q}|^3 \frac{M_{\Lambda_c}}{M_{\Lambda_{c1;S}^*}} \end{aligned} \quad (23)$$

The unknown masses of the excited bottom baryons  $\Lambda_{b1;S}$  and  $\Lambda_{b1;S}^*$  are estimated from the heuristic relation:  $m_{\Lambda_{b1;S}^{(*)}} = m_{\Lambda_{c1;S}^{(*)}} + (m_{\Lambda_b^0} - m_{\Lambda_c^+})$ .

#### IV. RESULTS

We now present our numerical results for the strong and radiative transitions of heavy baryons. In Table III we list our results for the one-pion coupling constants. For comparison we also give the results of the Light-Front (LF) Quark Model [14] where the masses of light quarks are varied in the range  $m_{u(d)} = 280 \pm 60$  MeV and  $m_s = m_{u(d)} + 150$  MeV =  $430 \pm 60$  MeV. Our predictions for the one-pion coupling constants are in qualitative agreement with the Light-Front quark model prediction. As in the Light-Front quark model [14] the strength of single pion couplings of the charmed baryon ground-state to the antisymmetric P wave states are suppressed with respect to those of the symmetric multiplet. The coupling values calculated in the Light-Front approach show a strong dependence on the masses of the light quarks. The results of Ref. [14] are quite close to our results for the mass choice  $m_{u(d)} = 220$  MeV and  $m_s = 370$  MeV. However, such low values of the constituent quark masses are excluded from the analysis of the magnetic moments and charge radii of nucleons. The smaller value of  $f_{\Lambda_{c1;S}^* \Sigma_c \pi}$  is welcome when one compares the results for exclusive one-pion rates of the  $\Lambda_{c1;S}^*$  (see, Table IV) with experimental data [1]. It is seen that our predictions are consistent with current experimental estimates whereas the Light-Front model results lie above the experimental rates. Also our predictions for  $d$ -wave transitions can be seen to be consistent with the bound on the total rate of the  $\Lambda_{c1;S}^*$  by summing up the three exclusive one-pion rates of the  $\Lambda_{c1;S}^*$  and comparing the sums to the total experimental rate  $\Gamma(\Lambda_{c1;S}^*) < 1.9$  MeV. From the results of our model calculation we obtain  $\Gamma(\Lambda_{c1;S}^*) > 0.25 \pm 0.03$  MeV consistent with the experimental results. All our results for the one-pion decay rates of charm baryons are collected in Table IV. The uncertainties for the calculated rates reflect the experimental errors in the charm baryon masses (see, Table I). For comparison we have also listed the predictions of the Light-Front quark model [14] and experimental results, where available. More precise data on the one-pion transitions of the excited  $\Lambda_{c1;S}$  baryon states to the ground states will allow for a more detailed comparison with the model predictions of dynamical models such as described in our approach and in the Light-Front quark model.

A few comments should be done concerning the relations of RTQM results to other approaches. The first comment concerns the baryon one-pion coupling constants appearing in Eq. (18). The chiral formalism employed in [15] implies that all such constants are proportional to the factor  $1/f_\pi$  associated with the pion field. In RTQM approach they are described by Eq.(9) and are proportional to the pion-quark coupling  $g_\pi$  which is determined by the compositeness condition discussed in Sec.II. However, it appears that the Goldberger-Treiman relation  $g_\pi = 2m_q/f_\pi$  is valid with an accuracy of a few percent. Hence the pion constant  $f_\pi$  effectively appears as a dimensional parameter in our expressions for the baryon one-pion coupling constants.

The second comment concerns the relation of the RTQM approach to the constituent quark model based on the  $SU(4) \otimes O(3)$  symmetry for the light diquark system [11,12]. Exploiting this symmetry one can reduce the number of the effective coupling constants both for one-pion and one-photon transitions [11,12]. For example, the ratio of the two

coupling constants  $f_{\Lambda_{c1;S}\Sigma_c\pi}$  and  $f_{\Sigma_{c0;S}\Lambda_c\pi}$  that govern the  $s$ -wave transitions  $\Lambda_{c1;S} \rightarrow \Sigma_c\pi$  and  $\Sigma_{c0;S} \rightarrow \Lambda_c\pi$  is predicted to be  $f_{\Lambda_{c1;S}\Sigma_c\pi}/f_{\Sigma_{c0;S}\Lambda_c\pi} = -1/\sqrt{3}$  in the  $SU(4) \otimes O(3)$  model. We emphasize that the  $SU(4) \otimes O(3)$  symmetry is not realized in the RTQM approach. For instance, differing from the  $SU(4) \otimes O(3)$  approach the light diquark current in  $\Sigma_{c0;S}$ -baryon is not related to that in  $\Lambda_{c1;S}$  (see TABLE I). Yet, numerically the  $SU(4) \otimes O(3)$  relations are reproduced with an amazing accuracy of around 1%. For the two above processes  $\Lambda_{c1;S} \rightarrow \Sigma_c\pi$  and  $\Sigma_{c0;S} \rightarrow \Lambda_c\pi$  we find numerically  $f_{\Lambda_{c1;S}\Sigma_c\pi}/f_{\Sigma_{c0;S}\Lambda_c\pi} = -0.58$  almost identical to the ratio  $-1/\sqrt{3}$  in the  $SU(4) \otimes O(3)$  approach. Note that the  $SU(4) \otimes O(3)$  symmetry can be implemented explicitly in the RTQM by replacing the light quark propagator by a constant value and by modifying the spinor structure of the baryon-quark vertices as was demonstrated in [32].

Numerical results for the one-photon decay rates are listed in Table V. As for one-pion rates the errors in our rate values reflect the experimental errors in the charm baryon masses [1,5] (see Table I). For the sake of comparison we also list the results of the model calculations [17]- [20] mentioned earlier on. Our results are quite close to the results of the nonrelativistic quark model [16]. In [17] the coupling strengths were parameterized in terms of the unknown effective coupling parameters  $c_{RS}$  and  $c_{RT}$ . A first rough estimate of the unknown coupling parameters can be obtained by setting them equal to 1 on dimensional grounds [17]. As is evident from Table V such an estimate is basically supported by our dynamical calculation. We do not agree with the predictions on the charm and bottom p-wave decay rates of [20] except for the  $\Lambda_{b1;S}^* \rightarrow \Lambda_b^0\gamma$  rate where we are closer to the rate calculated in [20].

Recently the radiative decays of bottom baryons were studied with the use of the light-cone QCD sum rules [24] in the leading order of heavy quark effective theory. For the decay rates of the  $\Sigma_b$  and  $\Sigma_b^*$  baryons to  $\Lambda_b^0\gamma$  the authors of [24] obtained

$$\Gamma(\Sigma_b \rightarrow \Lambda_b\gamma) = \alpha_{\text{eff}} |\vec{q}|^3 \quad \text{and} \quad \Gamma(\Sigma_b^* \rightarrow \Lambda_b\gamma) = \alpha_{\text{eff}}^* |\vec{q}|^3$$

where the couplings  $\alpha_{\text{eff}}$  and  $\alpha_{\text{eff}}^*$  are approximately equal to each other. The authors of [24] quote  $\alpha_{\text{eff}} \approx \alpha_{\text{eff}}^* \approx 0.03 \text{ GeV}^{-2}$ . In order to compare our model results with the results in [24] we set  $M_{\Lambda_Q} = M_{\Sigma_Q}$  in Eq. (23). We then obtain  $\alpha_{\text{eff}} = 4f^2/(3\pi) \approx 0.015 \text{ GeV}^{-2}$  which is one-half of the prediction of Ref. [24].

One has to remark that the rate of the  $\Sigma_c^* \rightarrow \Sigma_c\gamma$  decay is suppressed in comparison with the rate of  $\Sigma_c^* \rightarrow \Lambda_c\gamma$  decay as

$$\frac{\Gamma(\Sigma_c^* \rightarrow \Sigma_c\gamma)}{\Gamma(\Sigma_c^* \rightarrow \Lambda_c\gamma)} = \frac{1}{3} \left( \frac{f_{\Sigma_c^*\Sigma_c\gamma}}{f_{\Sigma_c^*\Lambda_c\gamma}} \right)^2 \frac{M_{\Sigma_c}}{M_{\Lambda_c}} \left( \frac{M_{\Sigma_c}^2 - M_{\Sigma_c}^2}{M_{\Sigma_c}^2 - M_{\Lambda_c}^2} \right)^3 \approx 10^{-3} \quad (24)$$

This estimate coincides with the prediction of the constituent quark model [11,12].

## V. CONCLUSION

Using the same Relativistic Three-Quark Model (RTQM) employed before successfully in studies of semileptonic decays of heavy baryons [31], we have analyzed strong (one-pion) and radiative decays of heavy baryons. We have obtained predictions for the values of couplings of charmed baryons with pions and for the rates of the one-pion transitions

$B_c^i(p) \rightarrow B_c^f(p') + \pi(q)$ . We have compared our results with those obtained in Light-Front Quark-Model [14]. We found that as in the Light-Front quark model [14] the strength of single pion couplings of the charmed baryon ground-state to the antisymmetric P wave states are suppressed with respect to those of the symmetric multiplet.

We have also obtained predictions for the rates of the one-photon transitions  $B_Q^i(p) \rightarrow B_Q^f(p') + \gamma(q)$ . We have compared our results with the results of other model calculations [17]-[20]. Unfortunately, there is no data on the one-photon transitions yet to compare our results with. For the one-photon decays from the  $p$ -wave states  $\Lambda_{c1;S} \rightarrow \Lambda_c + \gamma$  and  $\Lambda_{c1;S}^* \rightarrow \Lambda_c + \gamma$  our predicted rates are one order of magnitude below the upper limits given by the experiments calling for an one-order of magnitude improvement on the experimental upper limits. Although the  $\Xi_c' \rightarrow \Xi_c + \gamma$  one-photon decays have now been seen [5] it will be close to impossible to obtain rate values for these decays because the  $\Xi_c'$ -states are far too narrow to be experimentally resolvable. The total widths of the  $\Sigma_c$ ,  $\Sigma_c^*$  and  $\Xi_c^*$  states are larger because of their strong decays via one-pion emission. In fact the widths of the  $\Sigma_c^{*++}$  and  $\Sigma_c^{*0}$  have been determined [1]. One can hope that one-pion branching ratios can be experimentally determined for the  $\Sigma_c$ ,  $\Sigma_c^*$  and  $\Xi_c^*$  one-photon decay modes in the near future. We are looking forward to compare the predictions of the Relativistic Three-Quark Model for the calculated rates with future experimental data.

## ACKNOWLEDGMENTS

M.A.I, V.E.L and A.G.R thank Mainz University for hospitality where a part of this work was completed. This work was supported in part by the Heisenberg-Landau Program and by the BMBF (Germany) under contract 06MZ865. J.G.K. acknowledges partial support by the BMBF (Germany) under contract 06MZ865.

## APPENDIX A: GAUGE INVARIANCE IN RTQM

In this Appendix we provide a detailed discussion of how gauge invariance is maintained in the one-photon transitions of excited charm baryon states. As an example we consider the decay  $\Lambda_{c1;S}^* \rightarrow \Lambda_c \gamma$ . To begin with we keep the heavy quark mass and the heavy baryon masses finite. The corresponding matrix element has the form

$$M_{inv}^\gamma(\Lambda_{c1;S}^* \rightarrow \Lambda_c \gamma) = \bar{u}(p') \Lambda^{\mu\nu}(p, p') u_\nu(p) \varepsilon_\mu^*(q) \quad (A1)$$

Here the vertex function  $\Lambda^{\mu\nu}(p, p')$  is given by the expression

$$\Lambda^{\mu\nu}(p, p') = \Lambda_{\Delta, Q}^{\mu\nu}(p, p') + \Lambda_{\Delta, q}^{\mu\nu}(p, p') + \Lambda_{lcd}^{\mu\nu}(p, p') + \Lambda_{ncd}^{\mu\nu}(p, p') + \Lambda_{pole}^{\mu\nu}(p, p') \quad (A2)$$

Here  $\Lambda_{\Delta, Q}^{\mu\nu}(p, p')$ ,  $\Lambda_{\Delta, q}^{\mu\nu}(p, p')$ ,  $\Lambda_{lcd}^{\mu\nu}(p, p')$ ,  $\Lambda_{ncd}^{\mu\nu}(p, p')$  and  $\Lambda_{pole}^{\mu\nu}(p, p')$  are the partial contributions coming from the triangle diagram with the photon emitted by the heavy quark line, the triangle diagrams with the photon emitted by the light quark lines, the "local contact" diagrams (lcd), the "nonlocal contact" diagrams (ncd) and the pole diagrams: their functional form is given by

$$\begin{aligned}
\Lambda_{\Delta,Q}^{\mu\nu}(p,p') &= e_Q g_{eff} \int \frac{d^4 k_1}{\pi^2 i} \int \frac{d^4 k_2}{4\pi^2 i} \tilde{F}_B^2(k_1, k_2, 0) S_Q(k_1 + p') \gamma^\mu S_Q(k_1 + p) k_1^\nu \\
&\quad \times \text{tr}[\gamma_5 S_q(k_1 + k_2) \gamma_5 S_q(k_2)] \\
\Lambda_{\Delta,q}^{\mu\nu}(p,p') &= e_q g_{eff} \int \frac{d^4 k_1}{\pi^2 i} \int \frac{d^4 k_2}{4\pi^2 i} \tilde{F}_B(k_1, k_2, 0) \tilde{F}_B(k_1, k_2, q) S_Q(k_1 + p) k_1^\nu \\
&\quad \times \text{tr}[\gamma_5 S_q(k_1 + k_2) \gamma_5 S_q(k_2 - q) \gamma^\mu S_q(k_2)] \\
\Lambda_{\text{lcd}}^{\mu\nu}(p,p') &= -g^{\mu\nu} e_q g_{eff} \int \frac{d^4 k_1}{\pi^2 i} \int \frac{d^4 k_2}{4\pi^2 i} \tilde{F}_B(k_1, k_2, 0) \tilde{F}_B(k_1, k_2, -q) S_Q(k_1 + p') \\
&\quad \times \text{tr}[\gamma_5 S_q(k_1 + k_2) \gamma_5 S_q(k_2)] \\
\Lambda_{\text{ncd}}^{\mu\nu}(p,p') &= e_q g_{eff} \int \frac{d^4 k_1}{\pi^2 i} \int \frac{d^4 k_2}{4\pi^2 i} \tilde{F}_B(k_1, k_2, 0) k_1^\nu \text{tr}[\gamma_5 S_q(k_1 + k_2) \gamma_5 S_q(k_2)] \\
&\quad \times [S_Q(k_1 + p)(k_1 - k_2 + q)^\mu \frac{\tilde{F}_B(k_1, k_2, 0) - \tilde{F}_B(k_1, k_2, q)}{(k_1 - k_2)q + q^2} \\
&\quad - S_Q(k_1 + p')(k_2 - k_1 + q)^\mu \frac{\tilde{F}_B(k_1, k_2, 0) - \tilde{F}_B(k_1, k_2, -q)}{(k_2 - k_1)q + q^2}] \\
\Lambda_{\text{pole}}^{\mu\nu}(p,p') &= (e_Q + e_q) g_{eff} \int \frac{d^4 k_1}{\pi^2 i} \int \frac{d^4 k_2}{4\pi^2 i} \tilde{F}_B^2(k_1, k_2, 0) k_1^\nu \text{tr}[\gamma_5 S_q(k_1 + k_2) \gamma_5 S_q(k_2)] \\
&\quad \times \left\{ \gamma^\mu \frac{1}{m_f - \not{p}} S_Q(k_1 + p) + S_Q(k_1 + p') \frac{1}{m_i - \not{p}'} \gamma^\mu \right\}
\end{aligned}$$

where  $m_i$  and  $m_f$  are the masses of the initial and the final baryons, respectively;  $e_Q = 2e/3$  is the charge of the  $c$ -quark,  $e_q = e_{q_1} + e_{q_2}$  is the sum of charges of the light quarks in the heavy baryon ( $e_q = e/3$  in the present case).

It is a straightforward exercise to proof that the matrix element  $M_{inv}^\gamma(\Lambda_{c1;S}^* \rightarrow \Lambda_c \gamma)$  is gauge invariant, i.e.  $q_\mu \cdot \bar{u}(p') \Lambda^{\mu\nu}(p, p') u_\nu(p) = 0$  when both initial and final baryons are on their mass-shell:  $\not{p} u(p) = m_i u(p)$  and  $\bar{u}(p') \not{p}' = \bar{u}(p') m_f$ . We make use of the well-known Ward-Takahashi identities

$$\not{q} = S_Q^{-1}(k + p') - S_Q^{-1}(k + p), \quad \not{q} = S_q^{-1}(k - q) - S_q^{-1}(k)$$

and obtain

$$\begin{aligned}
q_\mu \cdot \bar{u}(p') \Lambda_{\Delta,Q}^{\mu\nu}(p, p') u_\nu(p) &= e_Q g_{eff} \int \frac{d^4 k_1}{\pi^2 i} \int \frac{d^4 k_2}{4\pi^2 i} \tilde{F}_B^2(k_1, k_2, 0) k_1^\nu \text{tr}[\gamma_5 S_q(k_1 + k_2) \gamma_5 S_q(k_2)] \\
&\quad \times \bar{u}(p') [S_Q(k_1 + p) - S_Q(k_1 + p')] u_\nu(p) \\
q_\mu \cdot \bar{u}(p') \Lambda_{\Delta,q}^{\mu\nu}(p, p') u_\nu(p) &= e_q g_{eff} \int \frac{d^4 k_1}{\pi^2 i} \int \frac{d^4 k_2}{4\pi^2 i} \tilde{F}_B(k_1, k_2, 0) k_1^\nu \text{tr}[\gamma_5 S_q(k_1 + k_2) \gamma_5 S_q(k_2)] \\
&\quad \times \bar{u}(p') [\tilde{F}_B(k_1, k_2, q) S_Q(k_1 + p) - \tilde{F}_B(k_1, k_2, -q) S_Q(k_1 + p')] u_\nu(p) \\
&\quad + q^\nu e_q g_{eff} \int \frac{d^4 k_1}{\pi^2 i} \int \frac{d^4 k_2}{4\pi^2 i} \tilde{F}_B(k_1, k_2, 0) \tilde{F}_B(k_1, k_2, -q) \\
&\quad \times \text{tr}[\gamma_5 S_q(k_1 + k_2) \gamma_5 S_q(k_2)] \bar{u}(p') S_Q(k_1 + p') u_\nu(p) \\
q_\mu \cdot \bar{u}(p') \Lambda_{\text{lcd}}^{\mu\nu}(p, p') u_\nu(p) &= -q^\nu e_q g_{eff} \int \frac{d^4 k_1}{\pi^2 i} \int \frac{d^4 k_2}{4\pi^2 i} \tilde{F}_B(k_1, k_2, 0) \tilde{F}_B(k_1, k_2, -q) \\
&\quad \times \text{tr}[\gamma_5 S_q(k_1 + k_2) \gamma_5 S_q(k_2)] \bar{u}(p') S_Q(k_1 + p') u_\nu(p)
\end{aligned}$$



$$\begin{aligned}
q_\mu \cdot \bar{u}(p') \Lambda_{\text{ncd}}^{\mu\nu}(p, p') u(p) &= e_q g_{eff} \int \frac{d^4 k_1}{\pi^2 i} \int \frac{d^4 k_2}{4\pi^2 i} \tilde{F}_B(k_1, k_2, 0) k_1^\nu \text{tr}[\gamma_5 S_q(k_1 + k_2) \gamma_5 S_q(k_2)] \\
&\times \left\{ [\tilde{F}_B(k_1, k_2, 0) - \tilde{F}_B(k_1, k_2, q)] \bar{u}(p') S_Q(k_1 + p) u_\nu(p) \right\} \\
&- [\tilde{F}_B(k_1, k_2, 0) - \tilde{F}_B(k_1, k_2, -q)] \bar{u}(p') S_Q(k_1 + p') u_\nu(p) \Big\} \\
q_\mu \cdot \bar{u}(p') \Lambda_{\text{pole}}^{\mu\nu}(p, p') u_\nu(p) &= (e_Q + e_q) g_{eff} \int \frac{d^4 k_1}{\pi^2 i} \int \frac{d^4 k_2}{4\pi^2 i} \tilde{F}_B^2(k_1, k_2, 0) k_1^\nu \\
&\times \text{tr}[\gamma_5 S_q(k_1 + k_2) \gamma_5 S_q(k_2)] \bar{u}(p') [S_Q(k_1 + p') - S_Q(k_1 + p)] u_\nu(p)
\end{aligned}$$

Summing up the five contributions we arrive at  $q_\mu \cdot \bar{u}(p') \Lambda^{\mu\nu}(p, p') u_\nu(p) = 0$ .

In the heavy quark limit, when the masses of the charm quark and the heavy baryons go to infinity, the triangle diagram where the photon is emitted by the heavy quark ( $\Lambda_{\Delta, Q}^{\mu\nu}(p, p')$ ) and the pole diagrams ( $\Lambda_{\text{pole}, Q}^{\mu\nu}(p, p')$ ) vanish as  $1/M$ . The sum of the remaining contributions  $\Lambda_{\Delta, q}^{\mu\nu}(p, p')$ ,  $\Lambda_{\text{lcd}, Q}^{\mu\nu}(p, p')$  and  $\Lambda_{\text{ncd}, Q}^{\mu\nu}(p, p')$  can be seen to have the following gauge-invariant Lorentz structure also appearing in Eq.(19)

$$\Lambda^{\mu\nu}(v, q) = F(g^{\mu\nu} v q - v^\mu q^\nu)$$

where  $F$  is an effective coupling constant of the charm baryons with the photon.

## REFERENCES

- [1] C. Caso et.al. (Particle Data Group), Eur. Phys. J. **C3** (1998) 1.
- [2] G. Brandenburg et.al., CLEO Coll., Phys. Rev. Lett **78**, 2304 (1997).
- [3] P. Avery et.al., CLEO Coll., Phys. Rev. Lett. **75**, 4364 (1995).
- [4] L. Gibbons et.al., CLEO Coll., Phys. Rev. Lett. **77**, 810 (1996).
- [5] T.E. Coan et al., CLEO Coll., Preprint CLEO CONF 97-29, 1997;  
P. Jessop et al., Phys. Rev. Lett. **82**, 492 (1999).
- [6] H. Albrecht et.al., ARGUS Coll., Phys. Lett. **B317**, 227 (1993);  
Phys. Lett. **B402**, 207 (1997).
- [7] P.L. Frabetti et.al, E687 Coll., Phys. Rev. Lett. **72**, 961 (1994);  
Phys. Lett B **365**, 461 (1996).
- [8] K.W. Edwards et.al., CLEO Coll., Phys. Rev. Lett. **74**, 3331 (1995).
- [9] G. Brandenburg et al., CLEO Coll., Preprint CLEO CONF 97-17, 1997.
- [10] J.G. Körner, M. Krämer, and D. Pirjol, Prog. in Part. Nucl. Phys. **33**, 787 (1994).
- [11] F. Hussain, J.G. Körner, J. Landgraf, and S. Tawfiq Z. Phys. **C69**, 655 (1996).
- [12] F. Hussain, J.G. Körner, and S. Tawfiq, Preprints MZ-TH/96-10, IC/96/35, 1996.
- [13] D. Pirjol and T.M. Yan, Phys. Rev. D **56**, 5483 (1997).
- [14] S. Tawfiq, P.J. O'Donnell, and J.G. Körner, Phys. Rev. **D58**, 054010 (1998);  
Preprint UTPT-98-08, 1998.
- [15] T.M. Yan et. al., Phys. Rev. **D46**, 1148 (1992).
- [16] H.-Y. Cheng et al. Phys. Rev. **D47**, 1030 (1993).
- [17] P. Cho, Phys. Rev. **D50**, 3295 (1994).
- [18] H.-Y. Cheng, Phys. Lett. **B399**, 281 (1997).
- [19] M.-Q. Huang, Y.-B. Dai, and C.-S. Huang, Phys. Rev. **D52**, 3986 (1995).
- [20] C.-K. Chow, Phys. Rev. **D54**, 3374 (1996).
- [21] G. Chiladze and A. Falk, Phys. Rev. **D56**, 6738 (1997).
- [22] M.J.Savage, Phys. Lett. **B345**, 61 (1995).
- [23] A.G. Grozin and O.I. Yakovlev, Eur. Phys. J. **C2**, 721 (1998).
- [24] S.-L. Zhu and Y.-B. Dai, hep-ph/9810243.
- [25] G.V. Efimov and M.A. Ivanov, "The Quark Confinement Model", IOP, 1993.
- [26] I.V. Anikin, M.A. Ivanov, N.B. Kulimanova and V.E. Lyubovitskij,  
Z. Phys. C **65**, 681 (1995); Phys. Atom. Nucl. **57**, 1021 (1994).
- [27] M.A. Ivanov and V.E. Lyubovitskij, Phys. Lett. **B408**, 435 (1997).
- [28] M.A. Ivanov, M.P. Locher, V.E. Lyubovitskij, Few-Body Syst. **21**, 131 (1996).
- [29] M.A. Ivanov and P. Santorelli, hep-ph/9903446.
- [30] A. Salam, Nuovo Cim. **25**, 224 (1962); S. Weinberg, Phys. Rev. **130**, 776 (1963).
- [31] M.A. Ivanov, V.E. Lyubovitskij, J.G. Körner and P. Kroll, Phys. Rev. **D56**, 348 (1997).
- [32] M.A. Ivanov, J.G. Körner, V.E. Lyubovitskij, and A.G. Rusetsky,  
Phys. Rev. **D57**, 5632 (1998); Mod. Phys. Lett. **A13**, 181 (1998).
- [33] M.A. Ivanov, J.G. Körner, V.E. Lyubovitskij, A.G. Rusetsky,  
Phys. Lett. **B442**, 435 (1998).
- [34] M.A. Ivanov, J.G. Körner, V.E. Lyubovitskij, Phys. Lett. **B448**, 143 (1999).
- [35] S. Mandelstam, Ann. Phys. **19**, 1 (1962).
- [36] J. Terning, Phys. Rev. **D44**, 887 (1991).

- [37] M.A. Ivanov, Yu.L. Kalinovsky, P. Maris, and C.D. Roberts,  
Phys. Rev. **C57**, 1991 (1998); Phys. Lett. **B416**, 29 (1998).

# TABLES

TABLE I. Quantum numbers of heavy baryons. ( $\lambda_u = \text{diag}(1, 0, 0)$ ,  $\lambda_d = \text{diag}(0, 1, 0)$ ,  $\overset{\leftrightarrow}{\partial}_\mu^\pm = \overset{\leftarrow}{\partial}_\mu \pm \overset{\rightarrow}{\partial}_\mu$ ).

Baryon	$J^P$	Quark Content	$\Gamma_1 \otimes C\Gamma_2$	$\lambda_{B_Q}$	Mass (MeV) [1]
$\Lambda_c^+$	$\frac{1}{2}^+$	c[ud]	$I \otimes C\gamma^5$	$i\lambda_2/2$	$2284.9 \pm 0.6$
$\Xi_c^+$	$\frac{1}{2}^+$	c[us]	$I \otimes C\gamma^5$	$i\lambda_5/2$	$2465.6 \pm 1.4$
$\Xi_c^0$	$\frac{1}{2}^+$	c[ds]	$I \otimes C\gamma^5$	$i\lambda_7/2$	$2470.3 \pm 1.8$
$\Xi_c^{+'}$	$\frac{1}{2}^+$	c{us}	$\gamma^\mu \gamma^5 \otimes C\gamma_\mu$	$\lambda_4/(2\sqrt{3})$	$2573.4 \pm 3.1$
$\Xi_c^{0'}$	$\frac{1}{2}^+$	c{ds}	$\gamma^\mu \gamma^5 \otimes C\gamma_\mu$	$\lambda_6/(2\sqrt{3})$	$2577.3 \pm 3.2$
$\Sigma_c^{++}$	$\frac{1}{2}^+$	c{uu}	$\gamma^\mu \gamma^5 \otimes C\gamma_\mu$	$\lambda_u/\sqrt{6}$	$2452.8 \pm 0.6$
$\Sigma_c^+$	$\frac{1}{2}^+$	c{ud}	$\gamma^\mu \gamma^5 \otimes C\gamma_\mu$	$\lambda_1/(2\sqrt{3})$	$2453.6 \pm 0.9$
$\Sigma_c^0$	$\frac{1}{2}^+$	c{dd}	$\gamma^\mu \gamma^5 \otimes C\gamma_\mu$	$\lambda_d/\sqrt{6}$	$2452.2 \pm 0.6$
$\Xi_c^{*+}$	$\frac{3}{2}^+$	c{us}	$I \otimes C\gamma_\mu$	$\lambda_4/2$	$2644.6 \pm 2.1$
$\Xi_c^{*0}$	$\frac{3}{2}^+$	c{ds}	$I \otimes C\gamma_\mu$	$\lambda_6/2$	$2643.8 \pm 1.8$
$\Sigma_c^{*++}$	$\frac{3}{2}^+$	c{uu}	$I \otimes C\gamma_\mu$	$\lambda_u/\sqrt{2}$	$2519.4 \pm 1.5$
$\Sigma_c^{*0}$	$\frac{3}{2}^+$	c{dd}	$I \otimes C\gamma_\mu$	$\lambda_d/\sqrt{2}$	$2517.5 \pm 1.4$
$\Lambda_{c1;S}$	$\frac{1}{2}^-$	c[ud]	$\gamma^\mu \gamma^5 \otimes C\gamma^5 \overset{\leftrightarrow}{\partial}_\mu^+$	$i\lambda_2/(2\sqrt{3})$	$2593.9 \pm 0.8$
$\Sigma_{c0;S}$	$\frac{1}{2}^-$	c{ud}	$I \otimes C\gamma^\mu \overset{\leftrightarrow}{\partial}_\mu^+$	$\lambda_1/(2\sqrt{3})$	2670
$\Sigma_{c1;A}$	$\frac{1}{2}^-$	c[ud]	$\gamma^\mu \gamma^5 \otimes C\gamma^5 \overset{\leftrightarrow}{\partial}_\mu^-$	$i\lambda_2/(2\sqrt{3})$	2670
$\Lambda_{c1;S}^*$	$\frac{3}{2}^-$	c[ud]	$I \otimes C\gamma^5 \overset{\leftrightarrow}{\partial}_\mu^+$	$i\lambda_2/2$	$2626.6 \pm 0.8$
$\Xi_{c1;S}^*$	$\frac{3}{2}^-$	c[us]	$I \otimes C\gamma^5 \overset{\leftrightarrow}{\partial}_\mu^+$	$i\lambda_5/2$	$2815.0 \pm 2.1$
$\Sigma_{c1;A}^*$	$\frac{3}{2}^-$	c[ud]	$I \otimes C\gamma^5 \overset{\leftrightarrow}{\partial}_\mu^-$	$i\lambda_2/(2\sqrt{3})$	2701
$\Lambda_b$	$\frac{1}{2}^+$	b[ud]	$I \otimes C\gamma^5$	$i\lambda_2/2$	$5624 \pm 9$
$\Lambda_{b1;S}$	$\frac{1}{2}^+$	b[ud]	$\gamma^\mu \gamma^5 \otimes C\gamma^5 \overset{\leftrightarrow}{\partial}_\mu^+$	$i\lambda_2/(2\sqrt{3})$	$5933 \pm 10$
$\Lambda_{b1;S}^*$	$\frac{1}{2}^+$	b[ud]	$I \otimes C\gamma^5 \overset{\leftrightarrow}{\partial}_\mu^+$	$i\lambda_2/2$	$5966 \pm 10$

TABLE II. Flavor coefficients  $I_1$ ,  $I_3$  and  $f_1$ ,  $f_3$ .

Decay mode	$I_1$	$f_1$	Decay mode	$I_3$	$f_3$
$\Sigma_c^+ \rightarrow \Lambda_c \pi^0$	1	$\sqrt{3}/2$	$\Lambda_{c1}(2593) \rightarrow \Sigma_c^0 \pi^+$	1	$3/2$
$\Sigma_c^0 \rightarrow \Lambda_c \pi^-$	1	$\sqrt{3}/2$	$\Lambda_{c1}(2593) \rightarrow \Sigma_c^+ \pi^0$	1	$3/2$
$\Sigma_c^{++} \rightarrow \Lambda_c \pi^+$	1	$\sqrt{3}/2$	$\Lambda_{c1}(2593) \rightarrow \Sigma_c^{++} \pi^-$	1	$3/2$
$\Sigma_c^{*0} \rightarrow \Lambda_c \pi^-$	1	$1/2$	$\Sigma_{c1}^0(2670) \rightarrow \Sigma_c^+ \pi^-$	1	$3/2$
$\Sigma_c^{*++} \rightarrow \Lambda_c \pi^+$	1	$1/2$	$\Xi_{c1}^*(2815) \rightarrow \Xi_c^{*0} \pi^+$	$1/\sqrt{2}$	$1/2$
$\Xi_c^{*0} \rightarrow \Xi_c^0 \pi^0$	$1/2$	$1/2$	$\Xi_{c1}^*(2815) \rightarrow \Xi_c^{*+} \pi^0$	$1/2$	$1/2$
$\Xi_c^{*+} \rightarrow \Xi_c^+ \pi^-$	$1/\sqrt{2}$	$1/2$	$\Lambda_{c1}^*(2625) \rightarrow \Sigma_c^0 \pi^+$	1	$\sqrt{3}/2$
$\Xi_c^{*+} \rightarrow \Xi_c^0 \pi^+$	$1/\sqrt{2}$	$1/2$	$\Lambda_{c1}^*(2625) \rightarrow \Sigma_c^+ \pi^0$	1	$\sqrt{3}/2$
$\Xi_c^{*+} \rightarrow \Xi_c^+ \pi^0$	$1/2$	$1/2$	$\Lambda_{c1}^*(2625) \rightarrow \Sigma_c^{++} \pi^-$	1	$\sqrt{3}/2$
			$\Xi_{c1}^*(2815) \rightarrow \Xi_c^{*0'} \pi^+$	$1/\sqrt{2}$	$\sqrt{3}/2$
			$\Xi_{c1}^*(2815) \rightarrow \Xi_c^{*+'} \pi^0$	$1/2$	$\sqrt{3}/2$
			$\Sigma_{c1}^{*0}(2701) \rightarrow \Sigma_c^+ \pi^-$	1	$\sqrt{3}/2$

TABLE III. Charm baryon-pion couplings.

Coupling	Our	Ref. [14]
$g_{\Sigma_c \Lambda_c \pi}$	$8.88 \text{ GeV}^{-1}$	$6.51 \pm 0.35 \text{ GeV}^{-1}$
$g_{\Xi_c^* \Xi_c \pi}$	$8.34 \text{ GeV}^{-1}$	$6.585 \pm 0.375 \text{ GeV}^{-1}$
$f_{\Lambda_{c1}; S \Sigma_c \pi}$	0.52	$0.665 \pm 0.135$
$f_{\Xi_{c1}^*; S \Xi_c^* \pi}$	0.36	$0.45 \pm 0.13$
$f_{\Sigma_{c1}; A \Sigma_c \pi}$	0.07	$0.075 \pm 0.015$
$f_{\Lambda_{c1}^*; S \Sigma_c \pi}$	$21.5 \text{ GeV}^{-2}$	$50.85 \pm 14.25 \text{ GeV}^{-2}$
$f_{\Xi_{c1}^*; S \Xi_c' \pi}$	$20 \text{ GeV}^{-2}$	$32.25 \pm 8.15 \text{ GeV}^{-2}$
$f_{\Sigma_{c1}^*; A \Sigma_c' \pi}$	$0.50 \text{ GeV}^{-2}$	$0.75 \pm 0.15 \text{ GeV}^{-2}$

TABLE IV. Strong one-pion decay rates.

$B_Q \rightarrow B'_Q \pi$	Our	Ref. [14]	Experiment
P-wave transitions			
$\Sigma_c^+ \rightarrow \Lambda_c \pi^0$	$3.63 \pm 0.27$ MeV	$1.555 \pm 0.165$ MeV	
$\Sigma_c^0 \rightarrow \Lambda_c \pi^-$	$2.65 \pm 0.19$ MeV	$1.435 \pm 0.155$ MeV	
$\Sigma_c^{++} \rightarrow \Lambda_c \pi^+$	$2.85 \pm 0.19$ MeV	$1.505 \pm 0.165$ MeV	
$\Sigma_c^{*0} \rightarrow \Lambda_c \pi^-$	$21.21 \pm 0.81$ MeV	$11.365 \pm 1.215$ MeV	$13.0^{+3.7}_{-3.0}$ MeV
$\Sigma_c^{*++} \rightarrow \Lambda_c \pi^+$	$21.99 \pm 0.87$ MeV	$11.765 \pm 1.265$ MeV	$17.9^{+3.8}_{-3.2}$ MeV
$\Xi_c^{*0} \rightarrow \Xi_c^0 \pi^0$	$1.01 \pm 0.15$ MeV	$0.525 \pm 0.055$ MeV	
$\Xi_c^{*0} \rightarrow \Xi_c^+ \pi^-$	$2.11 \pm 0.29$ MeV	$1.30 \pm 0.15$ MeV	$\Gamma(\Xi^{*0}) < 5.5$ MeV
$\Xi_c^{*+} \rightarrow \Xi_c^0 \pi^+$	$1.78 \pm 0.33$ MeV	$1.09 \pm 0.12$ MeV	
$\Xi_c^{*+} \rightarrow \Xi_c^+ \pi^0$	$1.26 \pm 0.17$ MeV	$0.67 \pm 0.08$ MeV	$\Gamma(\Xi^{*+}) < 3.1$ MeV
S-wave transitions			
$\Lambda_{c1;S}(2593) \rightarrow \Sigma_c^0 \pi^+$	$0.83 \pm 0.09$ MeV	$1.775 \pm 0.695$ MeV	$0.86^{+0.73}_{-0.56}$ MeV
$\Lambda_{c1;S}(2593) \rightarrow \Sigma_c^+ \pi^0$	$0.98 \pm 0.12$ MeV	$1.18 \pm 0.46$ MeV	$\Gamma(\Lambda_{c1;S}) = 3.6^{+2.0}_{-1.3}$ MeV
$\Lambda_{c1;S}(2593) \rightarrow \Sigma_c^{++} \pi^-$	$0.79 \pm 0.09$ MeV	$1.47 \pm 0.57$ MeV	$0.86^{+0.73}_{-0.56}$ MeV
$\Xi_{c1;S}^*(2815) \rightarrow \Xi_c^{*0} \pi^+$	$0.46 \pm 0.03$ MeV	$1.575 \pm 0.835$ MeV	
$\Xi_{c1;S}^*(2815) \rightarrow \Xi_c^{*+} \pi^0$	$0.24 \pm 0.02$ MeV	$0.775 \pm 0.415$ MeV	$\Gamma(\Xi_{c1;S}^*) < 2.4$ MeV
$\Sigma_{c1;A}^0(2670) \rightarrow \Sigma_c^+ \pi^-$	$0.113 \pm 0.001$ MeV	$0.137 \pm 0.052$ MeV	
D-wave transitions			
$\Lambda_{c1;S}^*(2625) \rightarrow \Sigma_c^0 \pi^+$	$0.080 \pm 0.009$ MeV	$0.465 \pm 0.245$ MeV	$< 0.13$ MeV
$\Lambda_{c1;S}^*(2625) \rightarrow \Sigma_c^+ \pi^0$	$0.095 \pm 0.012$ MeV	$0.42 \pm 0.22$ MeV	$\Gamma(\Lambda_{c1}^*) < 1.9$ MeV
$\Lambda_{c1;S}^*(2625) \rightarrow \Sigma_c^{++} \pi^-$	$0.076 \pm 0.009$ MeV	$0.44 \pm 0.23$ MeV	$< 0.15$ MeV
$\Xi_{c1;S}^*(2815) \rightarrow \Xi_c^{*0} \pi^+$	$0.35 \pm 0.05$ MeV	$0.84 \pm 0.43$ MeV	
$\Xi_{c1;S}^*(2815) \rightarrow \Xi_c^{*+} \pi^0$	$0.21 \pm 0.03$ MeV	$0.435 \pm 0.205$ MeV	$\Gamma(\Xi_{c1}^*) < 2.4$ MeV
$\Sigma_{c1;A}^0(2701) \rightarrow \Sigma_c^+ \pi^-$	$0.0012 \pm 0.0001$ MeV	$0.0025 \pm 0.0015$ MeV	

TABLE V. Radiative decay rates

$B_Q \rightarrow B'_Q \gamma$	This approach	Other approaches	Experiment [1]
$\Sigma_c^+ \rightarrow \Lambda_c^+ \gamma$	$60.7 \pm 1.5$ KeV	93 KeV [16]	
$\Sigma_c^{*+} \rightarrow \Lambda_c^+ \gamma$	$151 \pm 4$ KeV		
$\Sigma_c^{*+} \rightarrow \Sigma_c^+ \gamma$	$0.14 \pm 0.004$ KeV		
$\Xi_c^+ \rightarrow \Xi_c^+ \gamma$	$12.7 \pm 1.5$ KeV	16 KeV [16]	
$\Xi_c^{\prime 0} \rightarrow \Xi_c^0 \gamma$	$0.17 \pm 0.02$ KeV	0.3 KeV [16]	
$\Xi_c^{*+} \rightarrow \Xi_c^+ \gamma$	$54 \pm 3$ KeV		
$\Xi_c^{\prime 0} \rightarrow \Xi_c^0 \gamma$	$0.68 \pm 0.04$ KeV		
$\Lambda_{c1;S}(2593) \rightarrow \Lambda_c^+ \gamma$	$0.115 \pm 0.001$ MeV	$0.191c_{RT}^2$ MeV [17] $0.016$ MeV [20]	$< 2.36_{-0.85}^{+1.31}$ MeV
$\Lambda_{c1;S}(2593) \rightarrow \Sigma_c^+ \gamma$	$0.077 \pm 0.001$ MeV	$0.127c_{RS}^2$ [17]	
$\Lambda_{c1;S}(2593) \rightarrow \Sigma_c^{*+} \gamma$	$0.006 \pm 0.0001$ MeV	$0.006c_{RS}^2$ [17]	
$\Lambda_{c1;S}^*(2625) \rightarrow \Lambda_c^+ \gamma$	$0.151 \pm 0.002$ MeV	$0.253c_{RT}^2$ MeV [17] $0.021$ MeV [20]	$< 1$ MeV
$\Lambda_{c1;S}^*(2625) \rightarrow \Sigma_c^+ \gamma$	$0.035 \pm 0.0005$ MeV	$0.058c_{RS}^2$ [17]	
$\Lambda_{c1;S}^*(2625) \rightarrow \Sigma_c^{*+} \gamma$	$0.046 \pm 0.0006$ MeV	$0.054c_{RS}^2$ [17]	
$\Xi_{c1;S}^{*+}(2815) \rightarrow \Xi_c^+ \gamma$	$0.190 \pm 0.005$ MeV		
$\Xi_{c1;S}^{\prime 0}(2815) \rightarrow \Xi_c^0 \gamma$	$0.497 \pm 0.014$ MeV		
$\Lambda_{b1;S}(5933) \rightarrow \Lambda_b^0 \gamma$	$0.128 \pm 0.022$ MeV	0.09 MeV [20]	
$\Lambda_{b1;S}^*(5966) \rightarrow \Lambda_b^0 \gamma$	$0.172 \pm 0.026$ MeV	0.119 MeV [20]	

# FIGURES

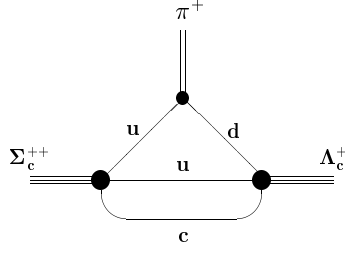


FIG. 1. Triangle diagram with a pion emitted by light quark.

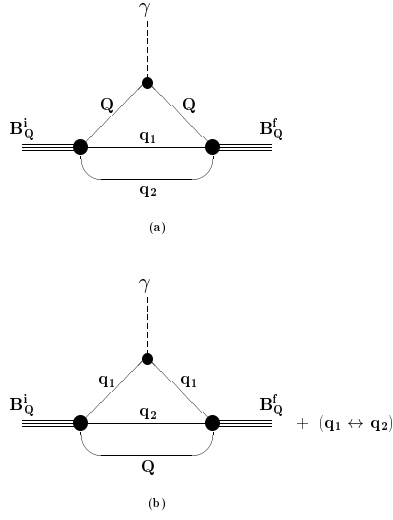


FIG. 2. Triangle diagrams with a photon emitted by (a) heavy and (b) light quark.



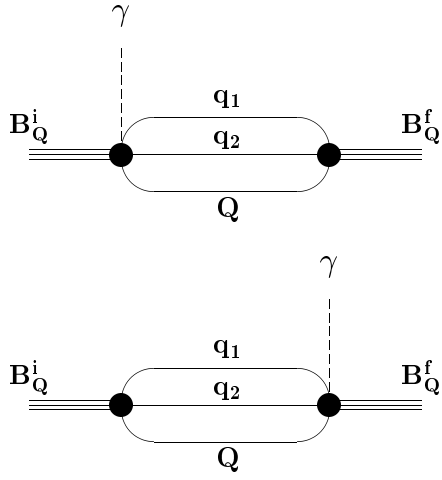


FIG. 3. Contact interaction-type diagrams.

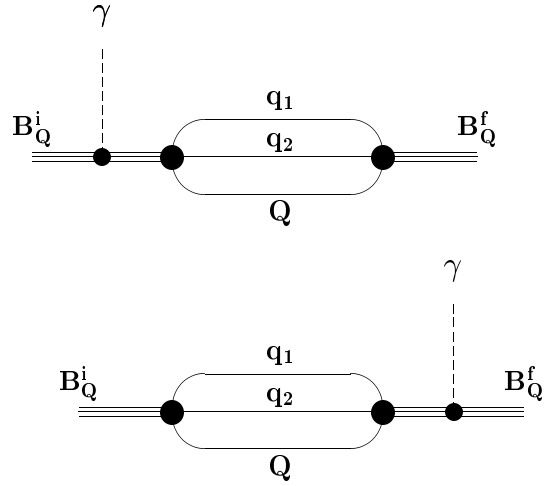


FIG. 4. Pole diagrams.